inter-noise 2008 From Silence to Harmony
37th International Congress and Exposition on Noise Control Engineering
26-29 October 2008·Shanghai·China

Recent developments in Direct Noise Computation of turbulent flows: numerical methods and applications

Christophe Bogey[a], Christophe Bailly[b]
[a] Laboratoire de Mécanique des Fluides et d'Acoustique, UMR CNRS 5509,
Ecole Centrale de Lyon, 69134 Ecully Cedex, France
[b] Same address & Institut Universitaire de France

ABSTRACT

The need of accurate and efficient numerical solvers in computational aeroacoustics has motivated the development over the last two decades of low-dispersion and low-dissipation schemes as an alternative to standard methods of computational fluid mechanics. These numerical methods have now reached maturity, even if progress is still necessary to take account of specific configurations. The present paper provides a short overview of some recent developments and applications of these methods, and is organized as follows. Motivations and numerical advances are first considered. Then the paper focuses on the use of direct noise simulations to improve our understanding of sound generation by turbulent flows. Applications to subsonic and supersonic jet noise are presented.

1 INTRODUCTION

The spectacular development of computational aeroacoustics since the early nineties has allowed the emergence of the direct computation of aerodynamic noise. There is still a lot of scope for progress, in particular for the numerical methods and for the applications to more complex configurations, but Direct Noise Computation (DNC) is currently a reliable and accurate tool, which can reproduce studied physics with high fidelity. DNC consists in solving the compressible Navier-Stokes equations to determine simultaneously the aerodynamic field and the acoustic field in a same domain. This approach is quite different from more classical modellings in which aerodynamics and acoustics are decoupled, such as the Lighthill analogy. It is consequently rather natural to apply this approach for studying in great detail noise mechanisms and modellings, and for evaluating noise reduction solutions. The resolution of more theoretical problems concerning aeroacoustics and propagation in the presence of a flow can also be performed by this way. Recent excellent technical reviews on computational aeroacoustics have moreover been written by Colonius and Lele [1], Wang *et al.* [2] or by Colonius [3] for the key problem of non-reflecting boundary conditions.

In the present paper, the constant progress in numerical methods is outlined in section 2 by the presentation of an optimized low-storage 4th-order Runge-Kutta scheme for which the dissipation error is significantly reduced. Section 3 is devoted to noise radiated by round subsonic jets, and thus to broadband noise associated with high-Reynolds-number turbulent free shear flows. The analysis of noise sources by a causality method is illustrated. In section 4, the noise radiated by a planar imperfectly expanded supersonic jet is discussed. In this case, the presence of a feedback mechanism introduces a frequency selection. The involved scales,

[a] Email address: christophe.bogey@ec-lyon.fr
[b] Email address: christophe.bailly@ec-lyon.fr

namely the scales associated with shocks, turbulence and acoustics are also strongly disparate. Concluding remarks and works in progress are finally provided.

2 NUMERICAL METHODS

The algorithms used for Direct Noise Computation require a continuous effort of development to improve numerical efficiency, allowing us to deal with more complex physical and geometrical configurations. A review of the use of finite-difference schemes is for instance available in Bailly & Bogey [4].

As an example of recent development which could significantly improve the accuracy of numerical simulations, the optimized Runge-Kutta scheme developed by Berland *et al.* [5] is now presented. This point illustrates the effort made in the development of low-dispersion and low-dissipation schemes for solving unsteady problems in fluid mechanics.

Consider the following semi-discrete differential equation

$$\frac{\partial u^n}{\partial t} = F\left(u^n, t\right)$$

where $u^n(x) = u(x, n\Delta t)$. From the time Fourier transform defined as

$$u(t) = \int_{-\infty}^{+\infty} \hat{u}(\omega) \exp(-i\omega t) d\omega$$

an amplification factor $R_s = \hat{u}^{n+1} / \hat{u}^n$ can be calculated. The integration error is then estimated by comparison between the exact amplification factor given by $R_e = \exp(-i\omega\Delta t)$ and the effective amplification factor of the scheme, which takes the following form

$$R_s = 1 + \sum_{j=1}^{p} \gamma_j \left(-i\omega\Delta t\right)^j \qquad (1)$$

Stability requires an amplification rate so that $|R_s(\omega\Delta t)| < 1$, and the integration errors are measured by comparing $R_s = |R_s| \exp(-i\omega_s\Delta t)$ with the exact amplification factor R_e in terms of dissipation error with $1 - |R_s|$, and of phase error with $|\omega_s\Delta t - \omega\Delta t|/\pi$.

The amplification rates of some classical schemes are reported in Figure 1 as a function of the normalized angular frequency $\omega\Delta t$. For waves up to four points per wavelength, *i.e.* for $\omega\Delta t \leq \pi/2$, there is more than three orders of magnitude between the dissipation of the classical Runge-Kutta scheme and the optimized low-storage scheme of Berland *et al.* [5], both providing a formal 4th-order integration. Note also the good behavior of the optimized scheme for the phase error, and the large time-step range of stability, $\omega\Delta t < 3.82$, with respect to the classical Runge-Kutta scheme yielding $\omega\Delta t < 2.83$.

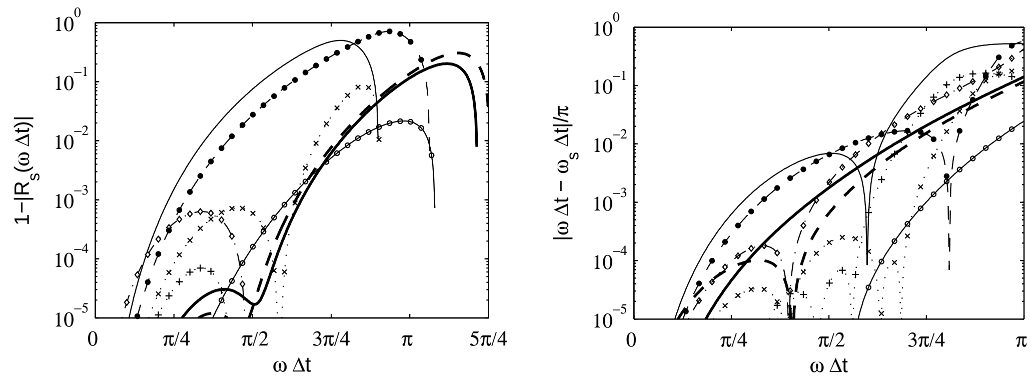

Figure 1: Modulus and phase error of the amplification factor (1) as a function of the angular frequency, in logarithmic scales: —— standard 4th-order RK algorithm, –o– standard 8th-order RK, + LDDRK46 Hu (1996), x LDDRK56 Hu (1996), –●– 4th-order 2N-RK Carpenter (1994), –◊– optimized. 4th-order 2N Stanescu (1998), ▬ ▬ optimized 2nd-order RK Bogey (2004), ▬▬ optimized 4th-order 2N-RK Berland (2006).

This example is reported to emphasize that new efficient algorithms have been developed over the last years, with the aim of controlling numerical dispersion and dissipation for solving unsteady nonlinear problems.

3 SUBSONIC JET NOISE

The prediction of subsonic jet noise is one of the oldest topics of aeroacoustics even if our understanding of noise mechanisms remains incomplete. The final goal of this research is the reduction of noise in urban environments. Indeed society cannot tolerate additional noise pollution, and traffic growth must be compensated by innovative noise reduction methods. This environmental challenge is also strategic for the economic development of the aeronautics industry. As pointed out in the introduction, the direct computation of aerodynamic noise using compressible large-eddy simulations is approaching maturity, and subsonic jet noise has been one of the first applications, with the direct numerical simulation (DNS) by Freund [6] of a jet at Mach number 0.9 and at Reynolds number based on the jet exit velocity and the jet diameter of 3600. The grid requirement of DNS is however difficult to satisfy for the computations of laboratory experiments with typical Reynolds number Re_D between 1e5 and 1e6. In addition, flow and noise characteristics are no longer dependent on the Reynolds number roughly for $Re_D \geq 2.5e5$. This observation is directly linked to the laminar or turbulent state of the nozzle exit boundary layer. Therefore, compressible Large Eddy Simulations (LES) appear relevant to develop DNC and to reproduce Reynolds number effects.

To illustrate this point, Figure 2 displays snapshots of the vorticity norm and of the fluctuating pressure for jets at Mach number 0.9 but at different Reynolds numbers in order to investigate the alterations on the flow development and on the radiated acoustic field. In the present work, the LES strategy is based on explicit selective filtering with spectral-like resolution combined with low-dispersion and low-dissipation numerical algorithms, see the discussion in Bogey and Bailly [7]. As the Reynolds number decreases, the jet flow changes significantly, and develops more slowly upstream of the end of the potential core, but more rapidly downstream.

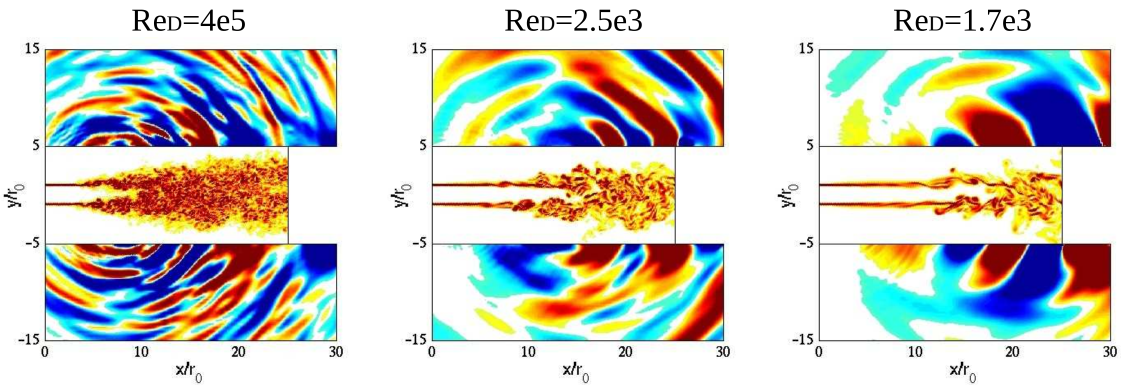

Figure 2: Jets at Mach M=0.9 and different Reynolds numbers. Snapshots of the vorticity norm in the flow and of the fluctuating pressure p' outside, in the plane z=0. The pressure color scale is p'=[-70, 70] Pa..

The acoustic field radiated in the sideline direction appears to vanish progressively as the Reynolds number is decreased, which can be directly linked to the absence of fine scale turbulence in the shear layers. Quantities such as mean velocity, jet spreading, turbulence intensity, integral length scales, spectra, acoustic azimuthal correlations and power laws have also been investigated as a function of the observer angle for circular jets at Mach number 0.6 and 0.9, with Reynolds numbers varying from 1.7e3 to 4e5 in Bogey and Bailly [8, 9]. The simulations suggest the presence of two sound sources: a Reynolds-number-dependent source, predominant for large radiation angles, connected to the randomly-developing turbulence, and a deterministic source, radiating downstream, related to a mechanism intrinsic to the jet geometry, which is still to be comprehensively described. This view agrees well with the experimental results displaying two distinguishable components in turbulent mixing noise.

Furthermore for the acoustic spectra of both components, a frequency scaling by a Strouhal number, St = fD/u_j, f being the frequency, D the jet diameter and u_j the jet velocity, appears suitable. However, the evolution of the peak is clearly different in the two directions, namely in the sideline direction and in the downstream direction. For observation angles $\theta \approx$ 90 deg., the spectral peak is Strouhal number dependent, and should be connected to the turbulence development in the shear layers between the nozzle and the end of the potential core. This evolution is also clearly visible on the spectral shape. In the downstream direction, the frequency peak is weakly dependent on the Reynolds number, with St $\approx$ 0.25, and this radiation can be linked to the periodic intrusion of vorticity at the end of the potential core.

The acoustic radiation by the turbulence developing in the shear layers seems partially understood, and active control or flow forcing by impinging micro-jets could be applied to achieve noise reduction. On the contrary, the noise mechanism at the end of the potential core is not well explained with our current knowledge of jet noise. Frequency selection of a global mode for subsonic cold jets is not predicted by the instability theory for instance, and is still to be clearly described. Based on this remark, it should be also underlined that there is still a role for theory, in particular to support the interpretation of these simulations.

Another possible way to establish direct links between turbulent flow events and emitted sound waves and to help towards the identification of noise-source mechanisms, is to apply a causality method to LES data, as proposed in Bogey and Bailly [9]. For that, the normalized cross-correlation between the jet turbulence at (x_1, t_0) and the radiated pressure at $(x_2, t_0 + t)$ is introduced

$$C_{fp}(x_1, x_2, t) = \frac{\left\langle f(x_1, t_0) p'(x_2, t_0 + t) \right\rangle}{\left\langle f^2(x_1, t_0) \right\rangle^{1/2} \left\langle p'^2(x_2, t_0) \right\rangle^{1/2}}$$

where the quantity f is any relevant calculated variable. Some results are reported in Figure 3 where f is the norm of the vorticity along the jet axis. The particular role played by the flow dynamic at the end of the potential core is again emphasized for the noise radiated in the downstream direction whatever the Reynolds number may be. This kind of investigation clearly needs more work using advanced signal processing and alternative localization techniques such as antenna or conditional statistics.

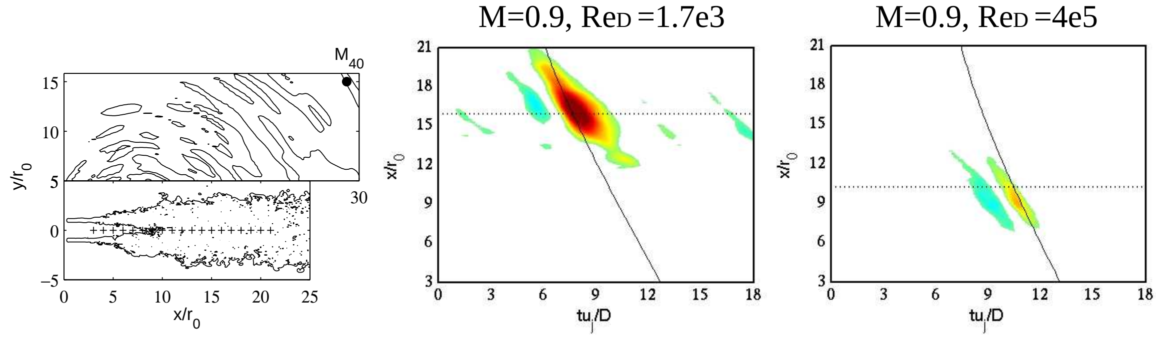

Figure 3: Correlations between the vorticity norms along the jet axis at points + and the acoustic field at point M_{40} indicated by ●. Time delay tu_j/D versus location x/r_0 along the jet axis, —— time of propagation along the acoustic rays, ….. end of the potential core, color scale: [-0.14 0.14] (white: [-0.035 0.035]).

To conclude and to provide a critical review, even if high-fidelity flow and noise simulations are now performed, it remains some difficulties such as the generation of artificial turbulence at the inflow boundary conditions to mimic the turbulent boundary layer or the thicker boundary layers used in numerical simulations, typically $\delta_\theta/D \approx$ 1e-2 instead of 1e-3 in experiments, leading to some potential shifts with measurements for the potential core length or spectral peaks in the initial shear-layer.

4 SUPERSONIC JET NOISE

Additional noise components generated by supersonic jets, and especially screech tones, contribute significantly to acoustic fatigue of combat aircrafts. Shock-associated noise radiates primarily in the upstream direction and consequently increases also notably cabin noise of modern commercial aircrafts. Noise of imperfectly expanded supersonic jets has been studied experimentally and theoretically in order to identify the interactions between turbulence and the quasi-periodic shock-cell structure. These interactions generate upstream-propagating sound waves. A resonant loop is then obtained when acoustic waves are diffracted by the nozzle lips and thus excite the initial shear layers. However, predictions are still qualitative and provide basically the fundamental frequency associated with the feedback loop. Further details can be found in the review paper of Raman [10]. The determination of the amplitude of the radiated acoustic field remains a difficult challenge, and is directly connected to a clear understanding of the shock - vortex interactions, as proposed by Suzuki and Lele [11] for the case of a planar shear layer.

This issue has been recently investigated by Berland *et al.* [12] with the compressible large eddy simulation of screech tones generated by a three-dimensional planar underexpanded jet. The jet operates at fully expanded Mach number M_j = 1.55, with a Reynolds number Re_h = 6e4 based on the jet exit velocity u_j and of the nozzle height h. The ratio between the exit pressure and the ambiant pressure is p_e/p_{amb} = 2.09, corresponding to maximum screech noise generated by a rectangular nozzle with large aspect ratio, as shown experimentally by Krothapalli et al. [13]. Numerical parameters and validations can be found in the paper previously mentioned. The flow and especially the shock-cell structure are in agreement with the literature. Furthermore the upstream acoustic field exhibits harmonic tones that compare correctly to screech tones observed on rectangular jets in terms of frequency, amplitude and phase shift on both sides of the jet.

As an illustration, Figure 4 displays a snapshot of the direct noise computation. Compression shocks corresponding to high-density gradients are seen inside the jet plume.

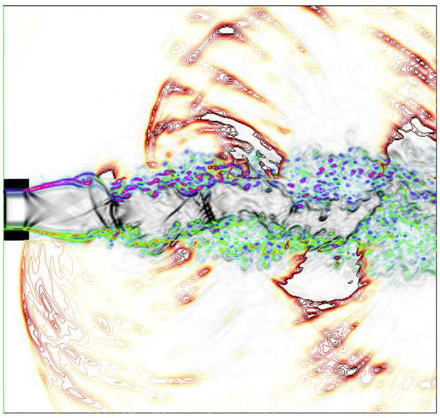

Figure 4: Computation of the generation of screech tones in an under-expanded supersonic jet, fully expanded jet at Mach number 1.55, Reynolds number 6e4.Snapshot of the density gradients, of the spanwise vorticity and of the near-field pressure, in a plane perpendicular to the spanwise direction. The nozzle lips are in black.

Upstream-propagating wave-fronts associated with screech tones radiation are clearly visible on both sides of the jet. The Strouhal number corresponding to the screech frequency is equal to $St = f_s h / u_j \approx 0.126$. A further study of the simulation data has permitted to locate the screech source near the third shock-cell, as noticed in the experiments of Krothapalli *et al.* [13] among others, and to provide evidences of the connection between the shock-leakage process, proposed by Suzuki and Lele [11] and the generation of screech tones.

The far-field noise is extrapolated by using the linearized Euler equations in order to compute acoustic spectra. Power spectral densities of the pressure fluctuations are reported in Figure 5 for different observation angles θ with respect to the downstream direction. Three contributions can be found: screech noise, broadband shock-associated noise and mixing noise which has already been discussed in the previous section devoted to subsonic jet noise. For θ = 155 deg., the spectrum is dominated by the fundamental screech tone and its harmonics. For an observer in the sideline direction, θ = 80 deg., the fundamental screech tone is no longer visible whereas its first harmonic dominates the radiated field. Two broadband peaks can also be noticed, a low-frequency contribution at $St \approx 0.07$ associated with the mixing noise and a higher frequency contribution over $0.1 \leq St \leq 0.2$. In the downstream direction, at θ = 40 deg., the mixing noise becomes the principal noise source.

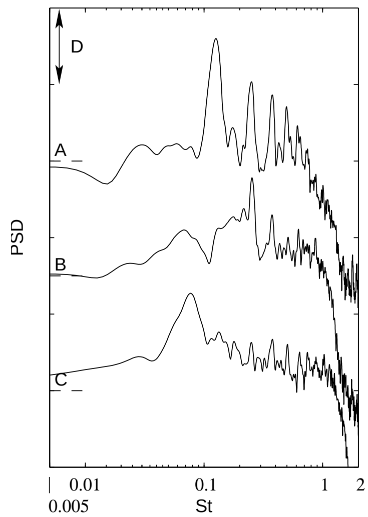

Figure 5: Computation of the generation of screech tones in an under-expanded supersonic jet, fully expanded at jet Mach number 1.55, Reynolds number 6e4. Far-field sound pressure spectra obtained at θ = 155 deg. (A), 80 deg. (B) and 40 deg. (C) with respect to the flow direction (D=10dB between two Y-ticks)

The present simulation is thus able to capture the three noise sources and to correctly reproduce broadband spectra as a function of the observer position, in agreement with the literature, as summarized by Raman [10] or by Tam [14].

5 CONCLUSIONS

Over the last years, significant progress has been done to improve the accuracy of Navier-Stokes solvers to perform Direct Noise Computation, in term of dissipation but also in term of dispersion for time-dependent simulations. It can be also observed that it is often easier to increase algorithm accuracy than the number of grid points of the mesh. And this recommendation also holds for commercial codes. DNC has also contributed to emphasize the role of silent boundary conditions combining non-reflecting outflow boundary conditions and sponge layers.

Turbulence modelling in large-eddy simulations remains a open key-issue for DNC, and needs to be objectively examinated with the knowledge of the transfer function of the numerical algorithm, as suggested by Domaradzki and Adams [15]. Simulation of realistic transitional shear layers at higher Reynolds numbers is still problematic and often leads to amplified local turbulence and noise sources. The methodology to specify the inflow boundary conditions of turbulent boundary layers in the framework of DNC likewise remains a challenging task, the reader may refer to Xu and Martin [16] for a recent discussion. Finally, validation and analysis of unsteady results, convergence of statistics for signal processing or comparison with low-resolved PIV data require precaution. Moreover, two-point space-time correlations are of particular importance for noise generation.

Among different topics in progress that can be mentioned, numerical study of more complex geometries involving high-Reynolds number flows requires the use of high-quality block structured grids. Several research teams develop such techniques with the aim of aeroacoustic simulations, as in Sherer and Scott [17]. Efforts are also now provided to develop unstructured approaches for realistic applications, even if accuracy and robustness seem still difficult and costly to preserve. Accuracy is also difficult to retain for transonic and supersonic flows in the context of aeroacoustics applications.

6 ACKNOWLEDGEMENTS

The authors would like to thank Julien Berland from SINUMEF, ENSAM Paris, for its contributions to this paper. The authors also gratefully acknowledge the Institut du Développement et des Ressources en Informatique Scientifique (IDRIS) of the CNRS and the Centre de Calcul Recherche et Technologie of the CEA (the French Atomic Energy Agency) for providing CPU time on Nec computers and technical assistance.

7 REFERENCES

[1] T. Colonius and S. Lele, “Computational aeroacoustics: progress on nonlinear problems on sound generation,” Progress in Aerospace Sciences, **40**, 345-416 (2004).

[2] T. Colonius, “Modeling artificial boundary conditions for compressible flows,” Annu. Rev. Fluid Mech., **36**, 315-345 (2004).

[3] M. Wang, J.B. Freund and S.K. Lele, “Computational prediction of flow-generated sound,” Annu. Rev. Fluid Mech., **38**, 483-512 (2006).

[4] C. Bailly and C. Bogey, “An overview of numerical methods for acoustic wave propagation,” *Proceedings of the European Conference of Computational Fluid Dynamics (2006)*, Paper 635.

[5] J. Berland, C. Bogey and C. Bailly, “Low-dissipation and low-dispersion fourth-order Runge-Kutta algorithm,” Computer & Fluids, **35**(10), 1459-1463 (2006).

[6] J.B. Freund, “Noise sources in a low-Reynolds-number turbulent jet at Mach 0.9, J. Fluid Mech.,” **438**, 277-305 (2001).

[7] C. Bogey and C. Bailly, “Large Eddy Simulations of transitional round jets: influence of the Reynolds number on flow development and energy dissipation,” Physics of Fluids, **18**, 065101, 1-14 (2006).

[8] C. Bogey and C. Bailly, “Investigation of downstream and sideline subsonic jet noise using Large Eddy Simulations,” Theoretical and Computational Fluid Dynamics, **20**(1), 23-40 (2006).

[9] C. Bogey and C. Bailly, “An analysis of the correlations between the turbulent flow and the sound pressure field of subsonic jets,” Journal of Fluid Mechanics, **583**, 71-97 (2007).

[10] G. Raman, “Supersonic jet screech: half-century from Powell to the present,” J. Sound Vib., **225**(3), 543-571 (1999).

[11] T. Suzuki and S. Lele, “Shock leakage through an unsteady vortex-laden mixing layer: application to screech jet,” Journal Fluid Mech., **490**, 139-167 (2003).
[12] J. Berland, C. Bogey and C. Bailly, “Numerical study of screech generation in a planar supersonic jet,” Phys. Fluids, **19**, 075105, 1-14 (2007).
[13] A. Krothapalli, Y. Hsia, D. Baganoff and K. Karamcheti, “The role of screech tones in mixing of an underexpanded rectangular jet,” J. Sound Vib., **106**(1), 119-143 (1986)
[14] C.K.W. Tam, “Supersonic jet noise,” Annu. Rev. Fluid Mech., **27**, 17-43 (1995).
[15] J.A. Domaradzki and N.A. Adams, “Direct modelling of subgrid scales of turbulence in large eddy simulations,” Journal of Turbulence, **3**(024), 1-19 (2002).
[16] S. Xu and M.P. Martin, “Assessment of inflow boundary conditions for compressible turbulent boundary layers,” Phys. Fluids, **16**(7), 2623-2639 (2004).
[17] S.E. Sherer and J.N. Scott, “High-order compact finite-difference methods on general overset grids,” J. Comput. Phys., **210**, 459-496 (2005).